

## **Polyaniline: The infrared spectroscopy of conducting polymer nanotubes (IUPAC Technical Report)\***

Miroslava Trchová<sup>‡</sup> and Jaroslav Stejskal

*Institute of Macromolecular Chemistry, Academy of Sciences of the Czech Republic, 162 06 Prague 6, Czech Republic*

*Abstract:* Polyaniline (PANI), a conducting polymer, was prepared by the oxidation of aniline with ammonium peroxydisulfate in various aqueous media. When the polymerization was carried out in the solution of strong (sulfuric) acid, a granular morphology of PANI was obtained. In the solutions of weak (acetic or succinic) acids or in water, PANI nanotubes were produced. The oxidation of aniline under alkaline conditions yielded aniline oligomers. Fourier transform infrared (FTIR) spectra of the oxidation products differ. A group of participants from 11 institutions in different countries recorded the FTIR spectra of PANI bases prepared from the samples obtained in the solutions of strong and weak acids and in alkaline medium within the framework of an IUPAC project. The aim of the project was to identify the differences in molecular structure of PANI and aniline oligomers and to relate them to supramolecular morphology, viz. the nanotube formation. The assignment of FTIR bands of aniline oxidation products is reported.

*Keywords:* aniline oligomers; Fourier transform infrared (FTIR) spectroscopy; IUPAC Polymer Division; nanotubes; polyaniline.

### **INTRODUCTION**

Polyaniline (PANI) is one of the most frequently studied conducting polymers with a wide application potential. PANI exists in variety of supramolecular morphologies [1]. PANI nanogranules are obtained when aniline is polymerized in strongly acidic aqueous media, which are currently used for the synthesis of a conducting PANI [2–4]. Oxidation in solutions of weak acids often produced PANI nanotubes. The first papers reporting their preparation were published by Wan et al. [5,6]. It has been proposed that weak organic acids present in the medium form salts with aniline. These have been assumed to organize into micelles and provide a soft template that guides the growth of nanotubes. Later, however, nanotubes have been synthesized in the absence of acids, just in water [7,8], and the role of a starting template was assigned to nanocrystallites produced by aniline oligomers, followed by helical nanotubular growth [9,10]. Nanosheets have been observed to accompany the nanotubes [8]. The self-curling of oligomer nanosheets to nanotubes has also been recently proposed [11]. PANI nanofibers should be mentioned as the next important morphology produced by aniline oxidation [12]. When aniline was oxidized in alkaline media, oligoaniline microspheres were formed [10,13].

---

\*Sponsoring body: IUPAC Polymer Division: see more details on page 1815. This publication resulted from work carried out under IUPAC Polymer Division Project 2006-018-2-400.

<sup>‡</sup>Corresponding author

The role of the initial acidity and the acidity profile during the oxidation of aniline were soon recognized to be a key factor in the formation of PANI nanostructures [7,10,14]. The growth of nanotubes was analyzed in detail by several research groups [1,9,14,15]. The formation of nanotubes in the oxidative polymerization of aniline with ammonium peroxydisulfate generally involves conditions of low initial acidity, i.e., the absence of added acid or the presence of weak organic acids in the reaction mixture [7–9,16]. It has been suggested that the molecular structure of the resulting material differs significantly from that of “standard polyaniline” [3], prepared under strongly acidic conditions. Aniline oligomers and their organized self-assemblies have been proposed to be responsible for the formation of one-dimensional nanostructures during the subsequent growth of PANI chains [10]. The problem thus reduces mainly to the elucidation of the molecular structure of the oxidation products, mainly those of an oligomeric nature, which predetermine the resulting supramolecular PANI morphology.

The molecular structure of the PANI samples of various morphologies obtained under different conditions may conveniently be studied by Fourier transform infrared (FTIR) spectroscopy, and several studies of this type have been reported in the literature [7–10,13,17–22]. The FTIR spectra of the final oxidation products prepared in media of various levels of acidity substantially differ from each other [10] (Fig. 1). The base forms of the oxidation products are generally better suited for the comparison of molecular structure, rather than their protonated counterparts, because the spectral features of counterions are absent. In addition to the main absorption bands of the PANI base, located at 1585 and 1497  $\text{cm}^{-1}$ , a shoulder at about 1630  $\text{cm}^{-1}$ , and bands at 1445 and 1414  $\text{cm}^{-1}$  are present in the spectra of the products obtained at low acidity and under alkaline conditions. It is supposed that they correspond to *o*-coupled aniline units and phenazine-like units [9]. These peaks are not visible in the spectra of PANI samples prepared in 0.1  $\text{mol}\cdot\text{dm}^{-3}$  sulfuric acid. The peak at 1374  $\text{cm}^{-1}$ , typical of a stan-

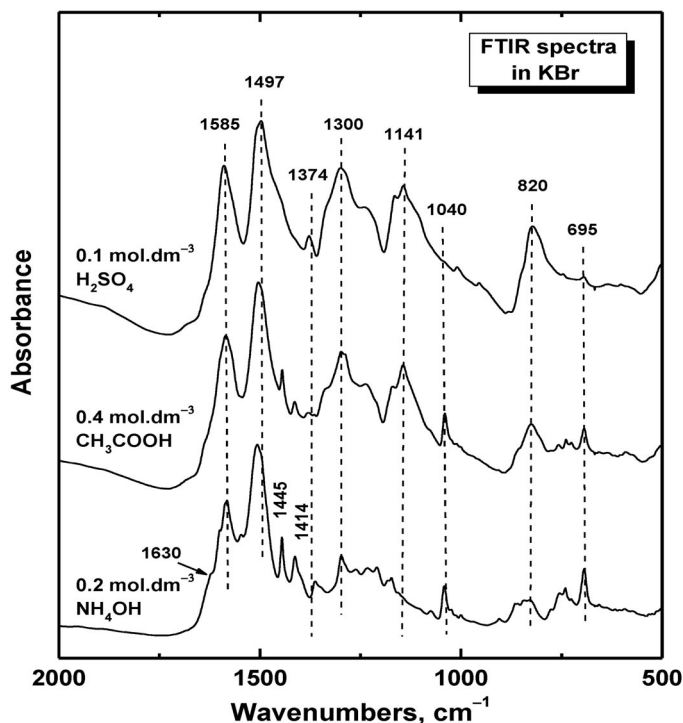


**Fig. 1** FTIR spectra of PANI (base form) obtained by the oxidation of aniline in strongly acidic medium (0.1  $\text{mol}\cdot\text{dm}^{-3}$  sulfuric acid), at low acidity (0.4  $\text{mol}\cdot\text{dm}^{-3}$  acetic acid), or under alkaline conditions (0.2  $\text{mol}\cdot\text{dm}^{-3}$  ammonium hydroxide) [10].

standard PANI base and assigned to C–N stretching in the neighborhood of a quinonoid ring [23], becomes smaller in the products prepared under less acidic conditions, e.g., in acetic acid solutions. The peak located at  $1040\text{ cm}^{-1}$  suggests the presence of sulfonate groups attached to the aromatic rings [8], but sulfate groups have also been proposed as an alternative [22].

The peaks described above have been observed in the FTIR spectra of nanostructured PANI prepared under various conditions by many authors [13,17–22]. Their interpretation and assignment, however, is still open to some discussion. They are also present in the first products of aniline oxidation [8,10,14,19,20,22,24] where aniline oligomers are expected to be generated [22,25,26]. The identification of early-stage intermediate species and their impact on the bulk polymer morphology is of substantial interest.

## PROJECT DESCRIPTION

The aim of the project 2006-018-2-400 “Infrared Spectroscopy of Conducting Polymer Nanotubes” was to find and confirm differences in molecular structure of the products of aniline oxidation at different levels of acidity and to relate them to supramolecular morphology, viz. nanotube formation. The products of aniline oxidation were therefore prepared and distributed to IUPAC project participants, and FTIR spectra were measured by experimentalists in various laboratories equipped with various spectrometers. The interpretation of the spectra was then jointly discussed.

## EXPERIMENTAL

### Preparation

The samples were prepared at the Institute of Macromolecular Chemistry (IMC), Academy of Sciences of the Czech Republic, by the oxidation of  $0.2\text{ mol}\cdot\text{dm}^{-3}$  aniline with  $0.25\text{ mol}\cdot\text{dm}^{-3}$  ammonium peroxydisulfate (Fig. 2) started at  $20\text{ }^{\circ}\text{C}$  in various media (Table 1). Commercial chemicals (Fluka, Switzerland; analytical grade) were used without purification. The reaction is exothermic, and the temperature rises to  $\approx 40\text{ }^{\circ}\text{C}$  during the preparation. The mixture was not stirred during the oxidation, which was complete within tens of minutes. The next day, the insoluble product was separated by filtration, rinsed with a solution of sulfuric, acetic, or succinic acid or with water. Portions of the isolated solids were deprotonated with an excess of  $1\text{ mol}\cdot\text{dm}^{-3}$  ammonium hydroxide to afford the bases (Fig. 3). The powders were dried at room temperature in air, and then in a desiccator over silica gel. The details of the preparation can be found elsewhere [7–10].

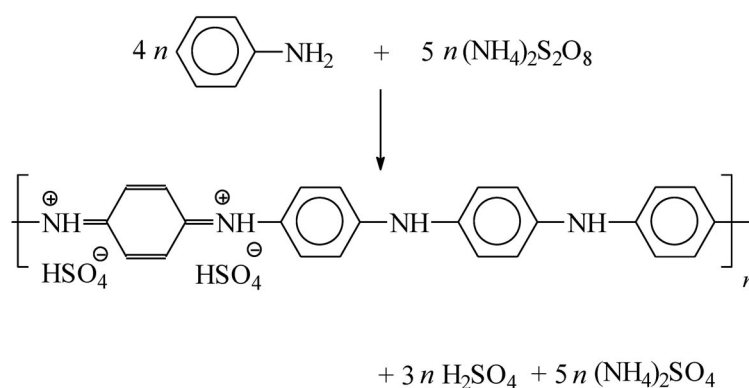


**Fig. 2** The oxidation of aniline with peroxydisulfate yields PANI hydrogen sulfate (or sulfate). Sulfuric acid and ammonium sulfate are by-products.

**Table 1** Codes of protonated forms and corresponding bases of aniline oxidation products prepared in aqueous media of various acidities, and used in the subsequent spectroscopic characterization.

Oxidation medium	Type	Sample code	
		Salt	Base
0.1 mol·dm <sup>-3</sup> Sulfuric acid	Strong acid	<i>H</i>	<i>H-B</i>
0.4 mol·dm <sup>-3</sup> Acetic acid	Weak acid	<i>Ac</i>	<i>Ac-B</i>
0.4 mol·dm <sup>-3</sup> Succinic acid	Weak acid	–	<i>Su-B</i>
Water	Neutral	–	<i>W-B</i>
0.2 mol·dm <sup>-3</sup> Ammonium hydroxide	Weak alkali	–	<i>Am 0.2-B</i>
1 mol·dm <sup>-3</sup> Ammonium hydroxide	Weak alkali	–	<i>Am 1-B</i>

### Properties

The morphology was assessed by electron microscopy [10]; under strongly acidic conditions, granules are produced, but nanotubes (Fig. 4) dominate in weakly acidic media, and microspheres are found in alkaline reaction mixtures (Table 2). The conductivity was determined by a four-point method on samples compressed into pellets of 13 mm diameter and 1 mm thickness; a two-point method was used for low-conductivity samples (Table 2). The conductivity decreases along with the acidity of the reaction medium. The density was determined by the Archimedes method by weighing the pellets in air and immersed in decane. The elemental composition was also determined (Table 3). The sample powders were then distributed to the individual project participants for spectroscopic characterization.

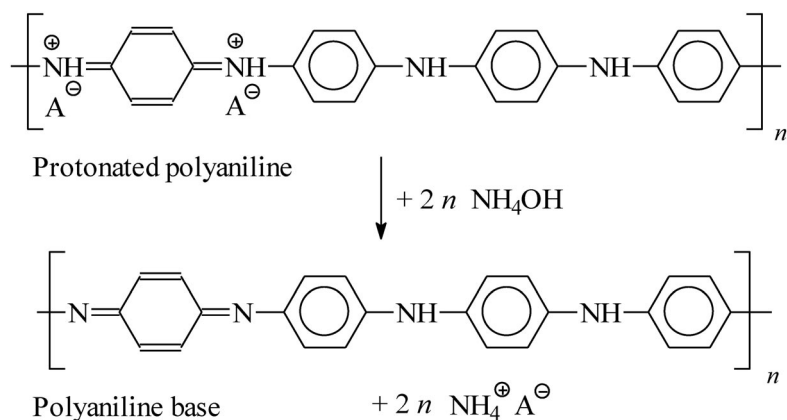


**Fig. 3** PANI (emeraldine) salt is deprotonated in alkaline medium to PANI (emeraldine) base. A<sup>-</sup> is an arbitrary anion, e.g., hydrogen sulfate.

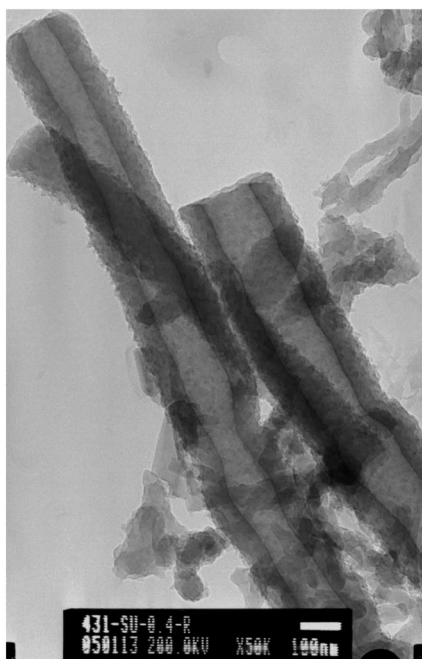


**Fig. 4** PANI nanotubes prepared in  $0.4 \text{ mol}\cdot\text{dm}^{-3}$  succinic acid.

**Table 2** Morphology, conductivity,  $\sigma$ , and density,  $d$ , of the protonated forms and the corresponding bases of aniline oxidation products prepared in aqueous media of various acidities.

Oxidation medium	Morphology	$\sigma/S\cdot\text{cm}^{-1}$		$d/g\cdot\text{cm}^{-3}$	
		Salt	Base	Salt	Base
$0.1 \text{ mol}\cdot\text{dm}^{-3}$ Sulfuric acid	Granular	1.3	$1.2 \times 10^{-9}$	1.40	1.23
$0.4 \text{ mol}\cdot\text{dm}^{-3}$ Acetic acid	Nanotubes	0.029	$7.9 \times 10^{-9}$	1.42	1.26
$0.4 \text{ mol}\cdot\text{dm}^{-3}$ Succinic acid	Nanotubes	0.059	$9.8 \times 10^{-9}$	1.37	1.26
Water	Nanosheets, nanotubes	$6.2 \times 10^{-3}$	$3.5 \times 10^{-9}$	1.41	1.25
$0.2 \text{ mol}\cdot\text{dm}^{-3}$ Ammonium hydroxide	Microspheres	(a)	$<10^{-10}$	(a)	–
$1 \text{ mol}\cdot\text{dm}^{-3}$ Ammonium hydroxide	Microspheres	(a)	$9.6 \times 10^{-13}$	(a)	–

<sup>a</sup>The samples were produced directly as bases.

**Table 3** Elemental composition (mass fraction) of aniline oxidation products prepared in aqueous media of various acidities and converted to bases.

Oxidation medium	C	H	N	S	O <sup>a</sup>
$0.1 \text{ mol}\cdot\text{dm}^{-3}$ Sulfuric acid	0.694	0.049	0.133	0.009	0.115
$0.4 \text{ mol}\cdot\text{dm}^{-3}$ Acetic acid	0.667	0.049	0.128	0.018	0.138
$0.4 \text{ mol}\cdot\text{dm}^{-3}$ Succinic acid	0.669	0.048	0.127	0.019	0.137
Water	0.669	0.048	0.128	0.020	0.135
$0.2 \text{ mol}\cdot\text{dm}^{-3}$ Ammonium hydroxide	0.683	0.048	0.132	0.020	0.117
$1 \text{ mol}\cdot\text{dm}^{-3}$ Ammonium hydroxide	0.701	0.049	0.150	0.013	0.087

<sup>a</sup>Calculated as difference from 1.

## RESULTS AND DISCUSSION

### FTIR spectra of samples measured in various laboratories

In conducting polymers, the incident infrared radiation interacts with vibrational excitations of the material and also with free carriers in their electronic structure. These interactions create phenomena such as free-carrier absorption, excitation across the energy gap, exciton transitions, or light-scattering by free electrons, and are reflected in the FTIR spectra. For studies of molecular structure, the attention has been centered especially on deprotonated samples, which are not influenced by acid molecules associated with the backbone (Fig. 3).

The methods of the measurements may influence the quality of the resulting spectra. This is impressively documented by the variability of the spectra published on PANI. The quality of IR spectra depends on sample preparation and on the performance of the instrumentation. Recommended conditions and parameters for the measurements were proposed to all the participants. The spectra were recorded on the FTIR spectrometers available in the participants' laboratories. The spectral region was adjusted to (400 to 4000)  $\text{cm}^{-1}$  and the spectral resolution was at a minimum of 4  $\text{cm}^{-1}$ . Detectors have been used as in routine measurements. The recommendation was made to measure by the transmission technique on PANI powders dispersed in potassium bromide pellets at the concentration and using the preparation methodology currently employed in the participating laboratories. Spectra might have been corrected for moisture and carbon dioxide in the optical path, while no other corrections should have been made unless specific details of such procedure were given. The spectra could be provided in the transmittance or absorbance version.

The spectra of two samples of PANI nanotubes, *Ac* and *Ac-B* (Table 1), measured in various laboratories, are compared in Figs. 5 and 6. The spectra differ when they are plotted in the whole region from (4000 to 500)  $\text{cm}^{-1}$ , and this may be caused by several factors; the influence of different ambient conditions (humidity, temperature, and pressure in sample preparation) and storing and processing of samples are some of them. The amount of moisture in the potassium bromide matrix varied in individual laboratories. The presence of the vibration bands of water molecules (at about 1630 and 3400  $\text{cm}^{-1}$ ) in most of the spectra (shown by arrows in Figs. 5 and 6) correspond to a higher humidity during measurement. The observed variability in the shape of the spectra of the *Ac* sample (especially above 2000  $\text{cm}^{-1}$ ) may be connected with the spontaneous deprotonation of PANI (Fig. 5a). The different sensitivity and quality of spectrometers (optics, detectors, etc.) have also influenced the spectra. The spectra of corresponding bases, *Ac-B*, are affected by moisture, but the positions and relative intensities of the main peaks are similar in the region below 2000  $\text{cm}^{-1}$  (Fig. 6b).

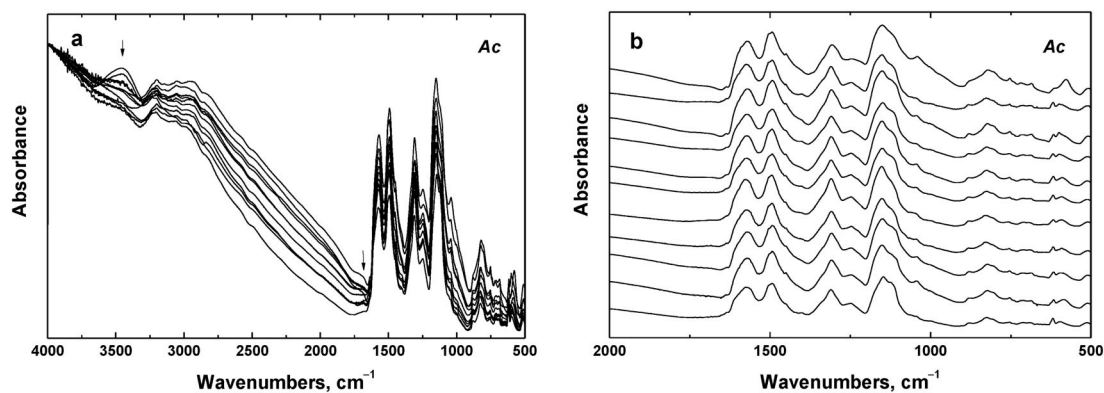


**Fig. 5** Comparison of the FTIR spectra of sample *Ac*, PANI nanotubes, in potassium bromide pellets, measured in various laboratories. (a) The spectra normalized at their absorption maxima and (b) vertically shifted for clarity.

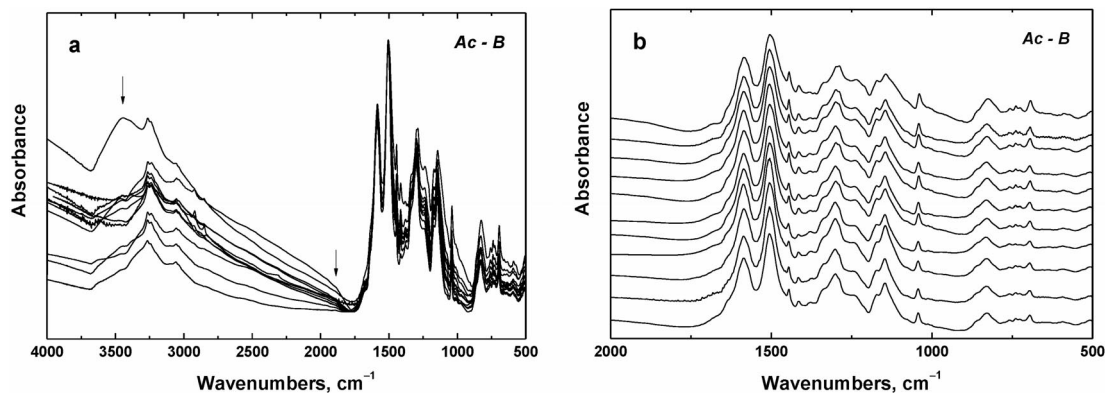


**Fig. 6** Comparison of the FTIR spectra of sample *Ac-B* in KBr pellets measured in various laboratories. (a) The spectra normalized at their absorption maxima and (b) vertically shifted for clarity.

### Processing and storage effects

In order to see the role of ageing under ambient conditions, we have measured fresh *Ac* and *Ac-B* samples (Figs. 7,8; spectrum 1) and the same samples after one year of storage in polyethylene bags under two different humidity conditions (spectra 2,3) at the IMC. In this case, the infrared spectra were recorded in the range of (400 to 4000)  $\text{cm}^{-1}$  at 64 scans per spectrum at 2  $\text{cm}^{-1}$  resolution, using a fully computerized Thermo Nicolet NEXUS 870 FTIR Spectrometer with a DTGS TEC detector. Measurements of the powdered samples were performed *ex situ* in the transmission mode in potassium bromide pellets. The spectra were corrected for moisture and carbon dioxide presence in the optical path.

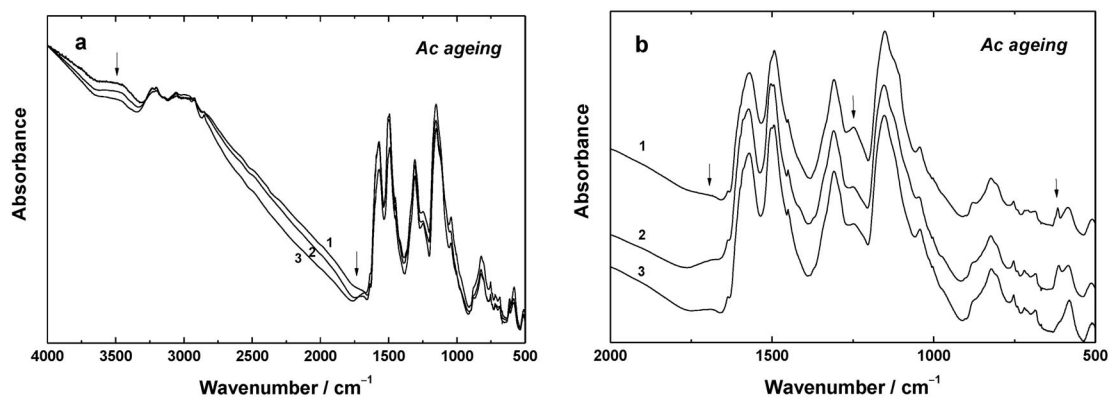


**Fig. 7** FTIR spectra of fresh sample *Ac* (1) measured at the IMC and the spectra measured after one year for two different humidity conditions (2,3). (a) The spectra normalized at their absorption maxima and (b) vertically shifted for clarity.

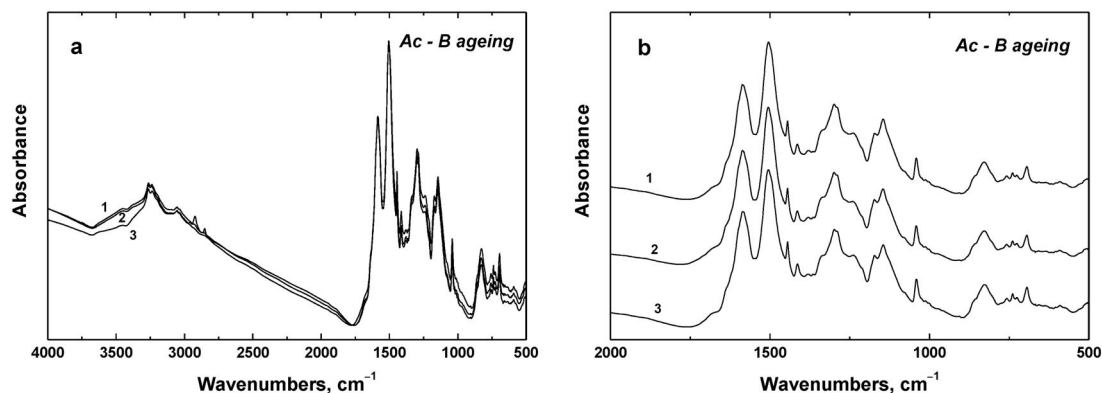


**Fig. 8** FTIR spectra of fresh sample *Ac-B* (1) measured at the IMC and the spectra measured after one year under two different humidity conditions (2,3). (a) The spectra normalized at their absorption maxima and (b) vertically shifted for clarity.

It was observed that the differences seen in the spectra (Fig. 7) are close to the differences observed in the spectra measured in different laboratories of the project participants (Fig. 5). It can be concluded that the different levels of humidity during the measurement are responsible for the variations in the spectra. We find that the positions of the peaks observed in the spectra of the deprotonated sample *Ac-B* are very close (Fig. 8). The same observation applies to all the samples distributed to the participants (Fig. 6). This may reflect the fact that the PANI base is much more hydrophobic than the corresponding protonated PANI [27].

### Interpretation of FTIR spectra

The full set of samples included two protonated PANIs and six bases (Table 1). Representative spectra of all fresh samples submitted by participants are presented in Figs. 9 and 10. The positions of the bands and peaks differed only within experimental error from the positions measured by individual participants. The interpretation of the spectra provided by the participants together with corresponding references proposed by the majority of them is summarized in Table 4. Open assignments, when the opinion of the participants differed, are set in boldface.

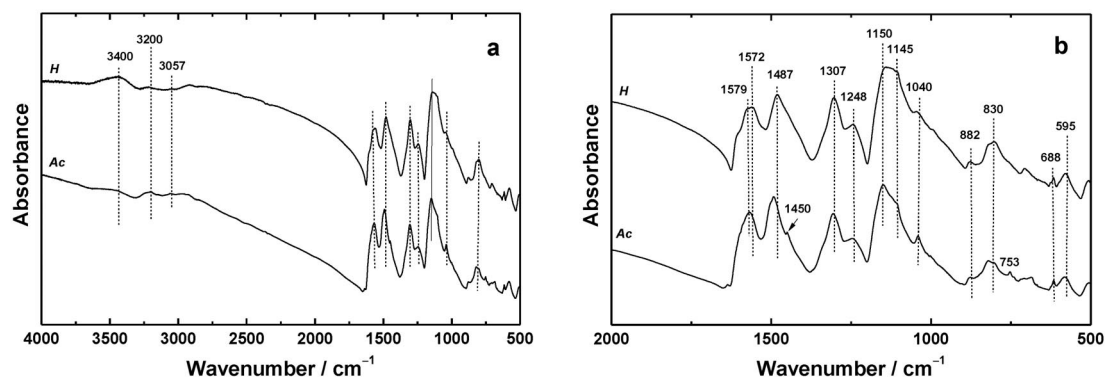


**Fig. 9** FTIR spectra of fresh protonated samples obtained at the IMC (a) over the whole wavenumber range, and (b) the detail between 500 and 2000  $\text{cm}^{-1}$ .

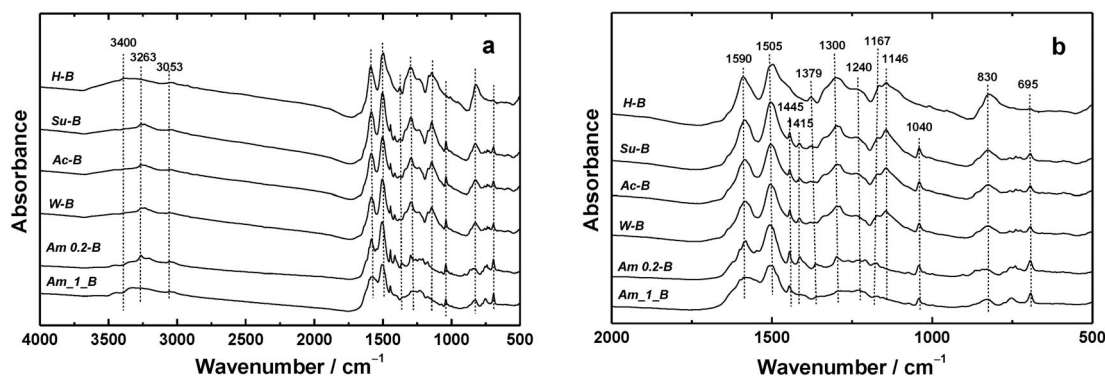


**Fig. 10** FTIR spectra of fresh bases obtained at the IMC (a) over the whole wavenumber range, and (b) the detail between 500 and 2000  $\text{cm}^{-1}$ .

**Table 4** Assignments of the IR bands for the aniline oxidation products prepared in aqueous media of various acidities.

Wavenumber/ $\text{cm}^{-1}$								Assignments
<i>H</i>	<i>H-B</i>	<i>Ac</i>	<i>Ac-B</i>	<i>Su-B</i>	<i>W-B</i>	<i>Am 0.2-B</i>	<i>Am 1-B</i>	
						1621 sh		N–H scissoring of primary aromatic amine/Phz [32,34]
1577 vs	1590 vs	1576 vs	1586 vs	1586 vs	1586 vs	1582 vs	1580 vs	Quinonoid (Q) ring-stretching [28,29]
						1547 s		Aromatic ring-stretching in substituted Phz unit [50,56]
1482 vs	1507 vs	1494 vs	1505 vs	1505 vs	1507 vs	1507 vs	1505 vs	Benzenoid (B) ring-stretching [28,29]
		<b>1451 m</b>	<b>1445 s</b>	<b>1445 s</b>	<b>1444 s</b>	<b>1445 s</b>	<b>1446 s</b>	<b>C=C stretching of aromatic ring [32,33]/</b>
		<b>1404 m</b>	<b>1415 s</b>	<b>1416 s</b>	<b>1415 s</b>	<b>1415 s</b>	<b>1415 s</b>	<b>N=N stretching</b>
		1379 m	1378 m	1379 m	1380 m			<b>Phz ring-stretching [8–10,15,50]</b>
			<b>1365 m</b>	<b>1366 m</b>	<b>1365 m</b>	<b>1364 m</b>		<b>C–N stretching in QBQ units [23,40]</b>
			1337 sh	1334 sh	1336 sh	1343 m	1347 s	<b>Stretching in Phz-type ring/v(C–N) [50,55,56]</b>
1307 vs	1305 vs	1310 vs	1299 s	1300/ 1290 s	1299/ 1289 s	1299 s	1287 s	v(C–N)
						1265 s	1272 sh	v(C–N) of secondary aromatic amine [23,40]
								v(C–N) of primary aromatic amine [33]
1248 s		1249 s						v(C–N <sup>+</sup> ) in the polaron lattice of PANI [41]
		1244 m	1238 s	1240 s	1240 s	1237 s	1231 s	v(C–N) in BBB unit [23]
						1210 s	1212 sh	Phz-type ring [8]
	<b>1167 s</b>		<b>1173 s</b>	<b>1173 s</b>	<b>1173 s</b>	<b>1173 s</b>	<b>1173 s</b>	<b>N=Q=N/<math>\delta</math>(C–H) [32,34]</b>
<b>1148 vs</b>		<b>1150 vs</b>						<b>Q=NH<sup>+</sup>–B or B–NH<sup>+</sup>–B [23,32,35,40,42–44]/</b>
								<b><math>\delta</math>(C–H)</b>
	1146 s		1145 s	1146 s	1146 s	1146 s	1155 s	B–NH–B/ $\delta$ (C–H) [23,32,45]

(continues on next page)

**Table 4** (Continued).

<i>H</i>	<i>H-B</i>	Wavenumber/cm <sup>-1</sup>						Assignments
		<i>Ac</i>	<i>Ac-B</i>	<i>Su-B</i>	<i>W-B</i>	<i>Am 0.2-B</i>	<i>Am 1-B</i>	
			1079 sh		1078 sh	1077 w-m	1073 m	δ(C-H) (monosubstituted ring) [32,33,56]
1045 sh		1042 sh	1041 s	1041 s	1041 s	1042 s	1042 s	H <sub>2</sub> SO <sub>4</sub> <sup>-</sup> /SO <sub>3</sub> <sup>-</sup> group on sulfonated aromatic ring [8-10,32,34,46,47]
					908 vw	907 w-m	902 w	γ(C-H) (1,2,4-trisubstituted ring) (1H) [8,32-34]
882 m		882 w-m			857 sh	867 s	868 sh	H <sub>2</sub> SO <sub>4</sub> <sup>-</sup> [32,34]
								γ(C-H) (1,2,4-trisubstituted ring) (2H) [8,32-34]/B ring deformation
<b>823 s</b>	<b>831 s</b>	<b>826 s</b>	<b>829 s</b>	<b>829 s</b>	<b>829 s</b>	<b>834 s</b>	<b>828 s</b>	<b>γ(C-H) (1,4-disubstituted ring) [23,32-34,40]/Q ring deformation</b>
		<b>753 w-m</b>	<b>760 m</b>	<b>760 m</b>	<b>759 w-m</b>	<b>757 m</b>	<b>754 s</b>	<b>γ(C-H) (monosubstituted or 1,2-disubstituted ring) [8,32-35,41,50]</b>
	695 w	688 w-m	695 s	695 m-s	695 m-s	696 s	693 s	Out-of-plane ring bending (monosubstituted ring) [32-35,40,41]
619 m		618 m						H <sub>2</sub> SO <sub>4</sub> <sup>-</sup> , SO <sub>4</sub> <sup>2-</sup> [32,48,49]
591 m-s		599 m	595 w-m	595 w	596 w	592 w	600 vw	H <sub>2</sub> SO <sub>4</sub> <sup>-</sup> [32,48,49]
The bands are masked by the "absorption tail".	3274		3262	3264	3264	3264	3438	v(N-H) (primary amino group) [30,32]
			3237	3238	3239		3315	v(N-H) [30,32]
		3200					3262	H-bonded v(N-H) [23,28-31]
								H-bonded v(N-H) [23,28-31]
							3204	H-bonded v(N-H) [23,28,31]
	<b>3051</b>	<b>3057</b>	<b>3054/3038</b>	<b>3054/3036</b>	<b>3054</b>	<b>3054/3037</b>	<b>3055/3033</b>	<b>Aromatic v(C-H) [32-34]/H-bonded v(N-H) [32-34]</b>

B: benzenoid ring; Q: quinonoid ring; Phz: phenazine; v: stretching; δ: in-plane deformation; γ: out-of-plane deformation; vs: very strong; s: strong; m: medium; w: weak; vw: very weak; sh: shoulder.

#### Granular PANI, samples *H* and *H-B*

The bands at 3274 and 3051 cm<sup>-1</sup> observed in the spectrum of deprotonated sample *H-B*, a PANI base (Fig. 10), are attributed to hydrogen-bonded N-H stretching [23,28-31] and aromatic C-H stretching [32-34], respectively (Fig. 3, Table 4). A broad absorption band at wavenumbers higher than 2000 cm<sup>-1</sup> in the spectrum of sample *H* (Fig. 9) is due to the absorption of free charge-carriers in the protonated polymer [29,35-38]. It is characteristic of a conducting form of PANI. A shoulder observed at 1610 cm<sup>-1</sup> in the spectrum of sample *H* is characteristic of C=C ring vibrations in the polymer chains whose symmetry has been broken by conformational changes induced by protonation [29]. The bands at 1577 and 1482 cm<sup>-1</sup> due to quinonoid (Q) and benzenoid (B) ring-stretching vibrations, respectively, observed in the spectrum of the sample *H* (protonated salt form), show a blue shift to 1590 and 1507 cm<sup>-1</sup>, respectively, in the spectrum of the corresponding base *H-B* [28,29]. The spectrum of *H-B*

exhibits the band at  $1379\text{ cm}^{-1}$ , typical for the PANI emeraldine base, attributed to C–N stretching vibration in the neighborhood of a quinonoid ring [23,39]. The absorption band at  $1307\text{ cm}^{-1}$  in the spectrum of the sample *H* corresponds to  $\pi$ -electron delocalization induced in the polymer by protonation [29]. This band is weaker in the spectrum of the corresponding base *H-B* and corresponds to the C–N stretching vibration of a secondary aromatic amine [23,40]. The band characteristic of the conducting protonated form is observed at  $1248\text{ cm}^{-1}$  in the spectrum of sample *H*. It has been interpreted as corresponding to a C–N<sup>+</sup> stretching vibration in the polaron structure [41].

The spectrum of the sample *H* exhibits a strong and broad band centered at  $1148\text{ cm}^{-1}$ , which has been assigned to the vibration mode of the  $-\text{NH}^+$  structure, and is associated with the vibrations of the charged polymer units  $\text{Q}=\text{NH}^+-\text{B}$  or  $\text{B}-\text{NH}^+-\text{B}$  [23,32,40]. This indicates the existence of positive charges on the chain and the distribution of the dihedral angle between the quinonoid and benzenoid rings. The absorption band increases with increasing degree of protonation of the PANI backbone [35,42]. This band has been related to the high degree of electron delocalization in PANI, as well as to a strong interchain  $\text{NH}^+\cdots\text{N}$  hydrogen bonding [43,44]. The asymmetric  $\text{SO}_3$  stretching vibration in the hydrogen sulfate counterion (Fig. 2) can also contribute to this band [32]. In contrast, the spectrum of a corresponding base *H-B* exhibits two sharp bands at  $1167$  and  $1146\text{ cm}^{-1}$  with much lower intensity. The former band corresponds to the mode of  $\text{N}=\text{Q}=\text{N}$  [23], and/or to the aromatic C–H in-plane deformation [32], and the latter to the mode  $\text{B}-\text{NH}-\text{B}$  and/or the aromatic C–H in-plane deformation [32]. The contribution of some remaining amount of charged polymer units to the last band is possible [45]. The shoulder observed at  $1045\text{ cm}^{-1}$  is attributable to the symmetric  $\text{SO}_3$  stretching in the hydrogen sulfate counterion. It is absent in the spectrum of the base *H-B* [8,32,34,46,47].

The band at  $882\text{ cm}^{-1}$  in the spectrum of the protonated sample *H* is absent in the spectrum of the base *H-B*. This band has been attributed to the  $\text{HSO}_4^-$  counterion, which was removed during the deprotonation [32,34] (Fig. 3). The most pronounced band at  $823\text{ cm}^{-1}$  in the substitution region ( $900$  to  $650$ )  $\text{cm}^{-1}$  in the spectrum of *H* is due to the C–H out-of-plane bending vibrations of two adjacent hydrogen atoms on a 1,4-disubstituted benzene ring [23,32–34,40]. This confirms the dominating *para*-coupling of constitutional units in PANI chains. After the deprotonation of the sample *H*, this band shifts to  $831\text{ cm}^{-1}$ . The bands observed at  $591$  and  $619\text{ cm}^{-1}$  in the spectrum of sample *H* are due to the hydrogen sulfate counterions; the latter band can be also attributed to sulfate counterions, which compete with those from hydrogen sulfate [32,48,49]. These bands are missing in the spectrum of deprotonated sample *H-B*.

#### Nanotubular samples *Ac*, *Ac-B*, *Su-B*

It should be kept in mind that the samples of this type are composed of two components, aniline oligomers and true PANI [10]. Depending on the mutual proportions, the FTIR spectra may somewhat vary. The differences between the spectra of granular PANI (*H*) and nanotubular products (*Ac*), thus reflect the presence of aniline oligomers. The product prepared in water (*W*) contains two-dimensional structures, such as nanoplates or micromats [9,14], in addition to nanotubes.

In comparison with the spectrum of the protonated sample *H*, the spectrum of the protonated sample *Ac* contains additional bands at wavenumbers ( $1451$ ,  $1404$ ,  $753$ , and  $688$ )  $\text{cm}^{-1}$  (Fig. 9, Table 4). The differences are even more pronounced in the spectra of the base forms, *H-B* and *Ac-B* (Fig. 10), and reflect differences in molecular structure and, consequently, in the granular vs. nanotubular morphologies of PANI synthesized in strongly and mildly acidic media, respectively. The spectrum of sample *Ac-B* contains new bands positioned at ( $1445$ ,  $1415$ ,  $1365$ ,  $1337$  (sh),  $1041$ ,  $760$ ,  $739$ ,  $728$ )  $\text{cm}^{-1}$ , which are absent in the spectrum of the granular base, *H-B* (Table 4).

The band at  $1445\text{ cm}^{-1}$  is attributed to the skeletal C=C stretching vibration of the aromatic ring [32–34]. It is difficult to assign precisely the position of substitution because of the overlapping frequency ranges for various types of substitution. Interpretation of this band is not unanimous, some of the participants suggest the presence of C=N stretching or N=N azobenzene stretching vibrations [32–34]. The peak at  $1415\text{ cm}^{-1}$  can be assigned to the ring-stretching of the phenazine constitutional

unit [8–10,15,50]. Such substituted phenazine constitutional units can be formed by the oxidative intramolecular cyclization of *o*-coupled aniline constitutional units or by the oxidative insertion of aniline molecule into *para*-linked aniline units [8,51–54]. The opinions of the participants on this band are not unanimous. A medium peak at  $1365\text{ cm}^{-1}$  corresponds to stretching vibrations in phenazine-type rings or to C–N stretching vibrations [50,55,56]. A shoulder at  $1337\text{ cm}^{-1}$  is attributed to C–N bonding [33], with the C atom belonging to the aromatic ring which is not simply *para*-substituted but probably 1,2,4-trisubstituted. It is known that the frequency of C–N stretching vibrations is largely determined by the aromatic character of the carbon atom [33]. The strong band at  $1299\text{ cm}^{-1}$  (for *Ac-B*) is due to the C–N stretching vibrations of aromatic amines [23,40] associated with *para*-linked aniline units, and is downshifted relative to the band at  $1305\text{ cm}^{-1}$  for the sample *H-B*. We observe a maximum at  $1167\text{ cm}^{-1}$ , which is primarily due to the aromatic C–H in-plane deformation and a sharper shoulder at  $1146\text{ cm}^{-1}$  in the spectrum of the sample *Ac-B*. As in the case of sample *H-B*, the former band corresponds to the mode N=Q=N and/or to the aromatic C–H in-plane deformation, and the latter is most probably due to the mode B–NH–B and/or the aromatic C–H in-plane deformation [23,32]. A new sharp band of medium-to-strong intensity at  $1041\text{ cm}^{-1}$  is observed in the spectrum of *Ac-B*, which can be attributed to the S=O stretching in sulfonate  $\text{SO}_3^-$  group substituting the aromatic ring [8–10].

The bands observed at  $760$  and  $695\text{ cm}^{-1}$  in the spectrum of *Ac-B* (at  $753$  and  $688\text{ cm}^{-1}$  for *Ac*) correspond to the C–H out-of-plane bending and the ring out-of-plane deformation of monosubstituted phenylene ring, respectively [8,32,33,35,41,50]. Increased intensity of the band at  $695\text{ cm}^{-1}$  in the spectrum of *Ac-B*, in comparison to the weak band at the same position in the spectrum of *H-B*, indicates a higher content of aniline oligomers bearing monosubstituted phenyl rings as terminal units and/or more pronounced branching of the chains in the nanotubular sample prepared in acetic acid in comparison to the sample *H*. The spectra of the samples *Su-B* and *W-B* are nearly identical with the spectrum of sample *Ac-B*, all samples being prepared in mildly acidic media.

#### *Oligomeric microspherical samples Am 0.2-B and Am 1-B*

The oxidations of aniline in alkaline media yield brown non-conducting oligomers. Aniline droplets serve as oxidation templates and, for that reason oligomers are often produced as microspheres [10]. Their branched structure was proposed to include the quinoneimine groups [22,26].

In comparison with the spectra of *Ac-B*, *Su-B*, and *W-B*, the spectrum of aniline oligomers prepared in alkaline medium [10], *Am 0.2-B*, contains new peaks at ( $1547$ ,  $1265$ ,  $1210$ ,  $1077$ , and  $907$ )  $\text{cm}^{-1}$  (Table 4). The spectrum of sample prepared with a higher concentration of ammonium hydroxide, *Am 1-B*, exhibits peaks at similar positions as *Am 0.2-B*, except for the  $1547\text{ cm}^{-1}$  peak which is absent (Table 4). The peak at  $1547\text{ cm}^{-1}$  can be attributed to the aromatic ring-stretching vibration in a substituted phenazine unit [50,56]. The characteristic band of the PANI emeraldine base at  $1379\text{ cm}^{-1}$  is not present in the spectra of *Am 0.2-B* and *Am 1-B*. The shoulder observed at  $\approx 1340\text{ cm}^{-1}$  in the spectra of samples prepared in mildly acidic and neutral media, assigned to C–N stretching, is transformed to a well-defined peak at  $1343$  and  $1347\text{ cm}^{-1}$  in the spectra of samples prepared under weakly alkaline conditions, *Am 0.2-B* and *Am 1-B*, respectively. This fact can be explained by the higher content of branched units in the samples *Am 0.2-B* and *Am 1-B*. The band due to the C–N stretching of a secondary amine, which typically occurs at  $\approx 1305\text{ cm}^{-1}$  in the spectra of standard PANI bearing predominately *p*-coupled units and is very strong for the sample *H*, is present in the spectrum of *Am 0.2-B* at  $1299\text{ cm}^{-1}$ . It is significantly weakened and shifted to  $1287\text{ cm}^{-1}$  in the spectrum of *Am 1-B*. In the range of C–N stretching vibrations, an additional band is observed at  $1265$  ( $1272$ )  $\text{cm}^{-1}$  in the spectrum of *Am 0.2-B* (*Am 1-B*), due to the C–N stretching vibration of a primary aromatic amine [33]. This band confirms the oligomeric nature of the oxidation products of aniline in an alkaline medium.

The high content of monosubstituted phenyl rings in samples prepared in ammonium hydroxide can be connected with the oligomeric nature of *Am 1-B* and *Am 0.2-B*, and also with the presence of *N*-phenylphenazine units in the oligomers [10]. A peak observed at  $867\text{ cm}^{-1}$  in the spectrum of *Am 0.2-B*, corresponding to the 1,2,4-trisubstitution pattern [8,32–34], is relatively much stronger than

a shoulder observed at  $857\text{ cm}^{-1}$  in the spectrum of *W-B*. This indicates more pronounced branching in the oxidation product *Am 0.2-B* synthesized in an alkaline medium. In contrast to all other spectra, the band at  $\approx 696\text{ cm}^{-1}$  is stronger than the band at  $\approx 830\text{ cm}^{-1}$  only in the spectra of *Am 0.2-B* and *Am 1-B*.

To conclude, the project participants agreed in the interpretation of most of the peaks observed in FTIR spectra. However, the assignment of the bands associated with the formation of PANI nanotubes is still open to discussion. The difficulty of determining the presence of specific complex organic structures from bands in the infrared spectra is due to the fact that they do not correspond to characteristic group frequencies. FTIR spectroscopy alone is not able to provide definite answers on the details of molecular structure [13,18,19]. Additional and complementary methods are thus needed to elucidate the molecular structures related to the formation of the PANI nanotubes.

## CONCLUSIONS

Depending on the acidity of the reaction medium used in the oxidation of aniline, the specific spectral features in the products have been identified. They are linked to the individual morphologies, viz. to the formation of granules, nanotubes, and microspheres, the one-dimensional nanotubular morphology being of prime interest. Their formation is connected with the generation of aniline oligomers that are able to self-assemble and later to guide the growth of nanotubes. The concrete molecular structure of the species that controls the growth of one-dimensional PANI objects, however, could not be specified. The role of phenazine-containing aniline oligomeric structures seems to be important in this respect. Well-designed synthetic experiments and the subsequent analysis employing other methods, such as Raman spectroscopy and NMR, are thus needed.

The project has illustrated that the nanostructures produced by conducting polymers, viz. PANI nanotubes, are of interest to many renowned research laboratories. The most positive result of the project can be seen in the stimulation of discussions and many additional experiments, which have recently been reviewed [57–59], and which will inspire future studies. A similar project based on the interpretation of Raman spectra is under consideration.

## MEMBERSHIP OF SPONSORING BODIES

Membership of the IUPAC Polymer Division Committee for the period 2010–2011 was as follows:

**President:** C. K. Ober (USA); **Vice President:** M. Buback (Germany); **Secretary:** M. Hess (Germany); **Titular Members:** D. J. Dijkstra (Germany); R. G. Jones (UK); P. Kubisa (Poland); G. T. Russell (Germany); M. Sawamoto (Japan); R. F. T. Stepto (UK); J.-P. Vairon (France); **Associate Members:** D. Berek (Slovakia); J. He (China); R. C. Hiorns (France); W. Mormann (Germany); D. W. Smith (USA); J. Stejskal (Czech Republic); **National Representatives:** K.-N. Chen (Taiwan); J.-S. Kim (Korea); G. Moad (Australia); M. Raza Shah (Pakistan); J. V. Seppälä (Finland); R. P. Singh (India); W. M. Z. B. Wan Yunus (Malaysia); Y. Yagci (Turkey); M. Zigon (Slovenia).

This publication resulted from work carried out under IUPAC Polymer Division Project 2006-018-2-400: **Task Group Members:** M. M. Ayad (Egypt); M. Bláha (Czech Republic); N. V. Blinova (Czech Republic); G. Ćirić-Marjanović (Serbia); M. Hasik (Poland); H. J. Choi (Korea); R. Holze (Germany); F. J. Huerta (Spain); E. N. Konyushenko (Czech Republic); J. Laska (Poland); P. Matějka (Czech Republic); P. Mokreva (Bulgaria); F. R. Montilla (Spain); M. Omastová (Slovakia); C. Quijada (Spain); S. Reynaud (France); H. J. Salavagione (Spain); I. Sapurina (Russia); B. Schulz (Germany); I. Šeděnková (Czech Republic); J. Stejskal (Czech Republic); L. Terlemezyan (Bulgaria); J. Travas-Sejdic (New Zealand); M. Trchová (*Task Group Leader*, Czech Republic); J. L. Vázquez (Spain); J. Vohlídal (Czech Republic); L. Zhang (New Zealand).

## ACKNOWLEDGMENTS

The participants wish to thank the IUPAC Polymer Division (IUPAC Project 2006-018-2-400) for encouragement and the Ministry of Education, Youths, and Sports of the Czech Republic (LA 09028) for financial support.

## REFERENCES

1. I. Sapurina, J. Stejskal. *Polym. Int.* **57**, 1295 (2008).
2. N. Gospodinova, P. Mokreva, L. Terlemezyan. *Polymer* **34**, 2438 (1993).
3. J. Stejskal, R. G. Gilbert. *Pure Appl. Chem.* **74**, 857 (2002).
4. J. Stejskal, I. Sapurina. *Pure Appl. Chem.* **77**, 815 (2005).
5. H. Qiu, M. Wan, B. Matthews, L. Dai. *Macromolecules* **34**, 675 (2001).
6. M. X. Wan. *Macromol. Rapid Commun.* **30**, 963 (2009).
7. E. N. Konyushenko, J. Stejskal, I. Šeděnková, M. Trchová, I. Sapurina, M. Cieslar, J. Prokeš. *Polym. Int.* **55**, 31 (2006).
8. M. Trchová, I. Šeděnková, E. N. Konyushenko, J. Stejskal, P. Holler, G. Ćirić-Marjanović. *J. Phys. Chem. B* **110**, 9461 (2006).
9. J. Stejskal, I. Sapurina, M. Trchová, E. N. Konyushenko, P. Holler. *Polymer* **47**, 8253 (2006).
10. J. Stejskal, I. Sapurina, M. Trchová, E. N. Konyushenko. *Macromolecules* **41**, 3530 (2008).
11. Y. F. Huang, C. W. Lin. *Polymer* **50**, 775 (2009).
12. D. Li, J. X. Huang, R. B. Kaner. *Acc. Chem. Res.* **42**, 135 (2009).
13. E. C. Venancio, P.-C. Wang, A. G. MacDiarmid. *Synth. Met.* **156**, 357 (2006).
14. C. Laslau, Z. D. Zujovic, L. J. Zhang, G. A. Bowmaker, J. Travas-Sejdic. *Chem. Mater.* **21**, 954 (2009).
15. A. Janošević, G. Ćirić-Marjanović, B. Marjanović, P. Holler, M. Trchová, J. Stejskal. *Nanotechnology* **19**, 135606 (2008).
16. E. N. Konyushenko, M. Trchová, J. Stejskal, I. Sapurina. *Chem. Pap.* **64**, 56 (2010).
17. C. M. S. Izumi, V. R. L. Constantino, M. L. A. Temperini. *J. Phys. Chem. B* **109**, 22131 (2005).
18. L. J. Zhang, H. Peng, Z. D. Zujovic, P. A. Kilmartin, J. Travas-Sejdic. *Macromol. Chem. Phys.* **208**, 1210 (2007).
19. Z. D. Zujovic, L. J. Zhang, G. A. Bowmaker, P. A. Kilmartin, J. Travas-Sejdic. *Macromolecules* **41**, 3125 (2008).
20. H. J. Ding, M. X. Wan. *Adv. Mater.* **19**, 465 (2007).
21. G. C. Li, C. Q. Zhang, H. R. Peng. *Macromol. Rapid Commun.* **29**, 63 (2008).
22. S. P. Surwade, V. Dua, N. Manohar, S. K. Manohar, E. Beck, J. P. Ferrari. *Synth. Met.* **159**, 445 (2009).
23. E. T. Kang, K. G. Neoh, K. L. Tan. *Prog. Polym. Sci.* **23**, 277 (1998).
24. L. J. Zhang, Z. D. Zujovic, H. Peng, G. A. Bowmaker, P. A. Kilmartin, J. Travas-Sejdic. *Macromolecules* **41**, 8877 (2008).
25. A. R. Hopkins, R. A. Lipeles, S.-J. Hwang. *Synth. Met.* **158**, 594 (2008).
26. J. Kříž, L. Starovoytova, M. Trchová, E. N. Konyushenko, J. Stejskal. *J. Phys. Chem. B* **113**, 6666 (2009).
27. J. Stejskal, J. Prokeš, M. Trchová. *React. Funct. Polym.* **68**, 1355 (2008).
28. Y. Furukawa, F. Ueda, Y. Hyodo, I. Harada, T. Nakajima, T. Kawagoe. *Macromolecules* **21**, 1297 (1988).
29. Z. Ping. *J. Chem. Soc., Faraday Trans.* **92**, 3063 (1996).
30. W. Zheng, M. Angelopoulos, A. J. Epstein, A. G. MacDiarmid. *Macromolecules* **30**, 2953 (1997).
31. I. Šeděnková, M. Trchová, N. V. Blinova, J. Stejskal. *Thin Solid Films* **515**, 1640 (2006).

32. G. Socrates. *Infrared and Raman Characteristic Group Frequencies*, pp. 107–113, 122–123, 157–167, 176–177, 220–222, John Wiley, New York (2001).
33. L. J. Bellamy. *The Infra-red Spectra of Complex Molecules*, pp. 65–84, 249–261, Richard Clay, Bungay, Suffolk (1962).
34. D. L. Vien, N. B. Colthup, W. G. Fateley, J. G. Grasselli. *The Handbook of Infrared and Raman Characteristic Frequencies of Organic Molecules*, pp. 277–299, Academic Press, San Diego (1991).
35. J. Tang, X. Jing, B. Wang, F. Wang. *Synth. Met.* **24**, 231 (1988).
36. A. J. Epstein, J. M. Ginder, F. Zuo, R. W. Bigelow, H. S. Woo, D. B. Tanner, A. F. Richter, W. S. Huang, A. G. MacDiarmid. *Synth. Met.* **16**, 303 (1986).
37. N. S. Sariciftci, H. Kuzmany, H. Neugebauer, A. Neckel. *J. Chem. Phys.* **92**, 4530 (1990).
38. K. G. Neoh, E. T. Kang, K. L. Tan. *Polymer* **34**, 3921 (1993).
39. E. T. Kang, K. G. Neoh, T. C. Tan, S. H. Khor, K. L. Tan. *Macromolecules* **23**, 2918 (1990).
40. M.-I. Boyer, S. Quillard, E. Rebourt, G. Louarn, J. P. Buisson, A. Monkman, S. Lefrant. *J. Phys. Chem. B* **102**, 7382 (1998).
41. M. L. Boyer, S. Quillard, G. Louarn, G. Froyer, S. Lefrant. *J. Phys. Chem. B* **104**, 8952 (2000).
42. J. C. Chiang, A. G. MacDiarmid. *Synth. Met.* **13**, 193 (1986).
43. M. Hasik, C. Paluszkiwicz, E. Wenda. *Vib. Spectrosc.* **29**, 191 (2002).
44. P. A. Colomban, A. Cruger, A. Novak, A. Regis. *J. Mol. Struct.* **317**, 261 (1994).
45. I. Šeděnková, J. Prokeš, M. Trchová, J. Stejskal. *Polym. Degrad. Stab.* **93**, 428 (2008).
46. Y. Şahin, K. Pekmez, A. Yıldız. *Synth. Met.* **131**, 7 (2002).
47. K. G. Neoh, M. Y. Pun, K. L. Tan. *Synth. Met.* **73**, 209 (1995).
48. N. V. Blinova, J. Stejskal, M. Trchová, G. Ćirić-Marjanović, I. Sapurina. *J. Phys. Chem. B* **111**, 2440 (2007).
49. M. M. Ayad, E. A. Zaki, J. Stejskal. *Thin Solid Films* **515**, 8381 (2007).
50. N. Neto, F. Ambrosino, S. Califano. *Spectrochim. Acta* **20**, 1503 (1964).
51. G. Ćirić-Marjanović, M. Trchová, J. Stejskal. *Collect. Czech. Chem. Commun.* **71**, 1407 (2006).
52. G. Ćirić-Marjanović, M. Trchová, J. Stejskal. *Int. J. Quantum Chem.* **108**, 318 (2008).
53. G. Ćirić-Marjanović, E. N. Konyushenko, M. Trchová, J. Stejskal. *Synth. Met.* **158**, 200 (2008).
54. G. Ćirić-Marjanović, M. Trchová, J. Stejskal. *J. Raman Spectrosc.* **39**, 1375 (2008).
55. G. Ćirić-Marjanović, M. Trchová, E. N. Konyushenko, P. Holler, J. Stejskal. *J. Phys. Chem. B* **112**, 6976 (2008).
56. G. Ćirić-Marjanović, N. V. Blinova, M. Trchová, J. Stejskal. *J. Phys. Chem. B* **111**, 2188 (2007).
57. C. Laslau, Z. Zujovic, J. Travas-Sejdic. *Prog. Polym. Sci.* **35**, 1403 (2010).
58. J. Stejskal, I. Sapurina, M. Trchová. *Prog. Polym. Sci.* **35**, 1420 (2010).
59. Y.-F. Huang, C.-W. Lin. *Polym. Int.* **59**, 1226 (2010).

---

Republication or reproduction of this report or its storage and/or dissemination by electronic means is permitted without the need for formal IUPAC permission on condition that an acknowledgment, with full reference to the source, along with use of the copyright symbol ©, the name IUPAC, and the year of publication, are prominently visible. Publication of a translation into another language is subject to the additional condition of prior approval from the relevant IUPAC National Adhering Organization.